

LETTER TO THE EDITOR

On the possible contributions of two nearby blazars to the NGC 4151 neutrino hotspot

A. Omeliukh^{1,*}, S. Barnier², and Y. Inoue^{2,3,4}

¹ Ruhr University Bochum, Faculty of Physics and Astronomy, Astronomical Institute (AIRUB), Universitätsstraße 150, 44801 Bochum, Germany

² Osaka University, Department of Earth and Space Science, Graduate School of Science, 1-1 Machikaneyama, Toyonaka, Osaka 560-0043, Japan

³ Interdisciplinary Theoretical & Mathematical Science Program (iTHEMS), RIKEN, 2-1 Hirosawa, Saitama 351-0198, Japan

⁴ Kavli Institute for the Physics and Mathematics of the Universe (WPI), UTIAS, The University of Tokyo, Kashiwa, Chiba 277-8583, Japan

Received XX; accepted XX

ABSTRACT

Context. The origin of the high-energy astrophysical neutrinos discovered by IceCube remains unclear, with both blazars and Seyfert galaxies emerging as potential sources. Recently, the IceCube Collaboration reported a $\sim 3\sigma$ neutrino signal from the direction of a nearby Seyfert galaxy NGC 4151. However, two gamma-ray loud BL Lac objects, 4FGL J1210.3+3928 and 4FGL J1211.6+3901, lie close to NGC 4151, at angular distances of 0.08° and 0.43° , respectively.

Aims. We investigate the potential contribution of these two blazars to the observed neutrino signal from the direction of NGC 4151 and assess their detectability with future neutrino observatories.

Methods. We model the multi-wavelength spectral energy distributions of both blazars using a self-consistent numerical radiation code, AM³. We calculate their neutrino spectra and compare them to the measured NGC 4151 neutrino spectrum and future neutrino detector sensitivities.

Results. Our models predict neutrino emission peaking at $\sim 10^{17}$ eV for both blazars, with fluxes of $\sim 10^{-12}$ erg cm⁻² s⁻¹. This indicates their contribution to the ~ 10 TeV neutrino signal observed from the direction of NGC 4151 is minor. While detection with current facilities is challenging, both sources should be detectable by future radio-based neutrino telescopes such as IceCube-Gen2's radio array and GRAND, with 4FGL J1210.3+3928 being the more promising candidate.

Key words. Neutrinos – Galaxies: BL Lacertae objects: individual – Methods: numerical – Radiation mechanisms: nonthermal

1. Introduction

More than ten years ago, the IceCube Neutrino Observatory discovered a diffuse flux of high-energy astrophysical neutrinos (IceCube Collaboration 2013), the nature of which still remains elusive. One of the most plausible candidates are blazars, a rare and energetic subclass of active galactic nuclei (AGNs). AGNs are powered by the accretion of matter onto supermassive black holes at the centers of galaxies. Blazars, distinguished by their relativistic jets aligned close to our line of sight, are natural candidates for neutrino emitters due to their role as powerful cosmic-ray accelerators. The blazar TXS 0506+056 was the first source associated with high-energy neutrino emission (IceCube Collaboration et al. 2018). IceCube has subsequently detected high-energy neutrino events in spatial and temporal coincidence with increased activity of several other individual blazars, among which are PKS 1424-41 (Kadler et al. 2016; Gao et al. 2017), GB6 J1040+0617 (Garrappa et al. 2019), PKS 1502+106 (Franckowiak et al. 2020; Rodrigues et al. 2021), and PKS 0735+178 (Sahakyan et al. 2022).

Recently, the landscape of potential neutrino sources has expanded beyond blazars to include other classes of AGNs. The IceCube Collaboration reported a 4.2σ signal from the nearby Seyfert galaxy, NGC 1068 (Aartsen et al. 2020; IceCube Collab-

oration et al. 2022). Seyfert galaxies, characterized by weak or absent jet activity, represent a distinct class of AGNs. Their coronal activity could produce gamma-ray deficit neutrinos (see e.g., Inoue et al. 2019). This potential has been further supported by additional observational studies (Abbasi et al. 2024a; Neronov et al. 2024; Sommani et al. 2024). The IceCube collaboration has recently announced a $\sim 3\sigma$ evidence for ~ 10 TeV neutrino emission from the direction of another Seyfert galaxy, NGC 4151 (Abbasi et al. 2024a,b). This nearby Seyfert galaxy, located at a distance of $d = 15.8$ Mpc (Yuan et al. 2020), provides an intriguing case study for investigating neutrino emission from Seyfert galaxies. Both corona and jet contributions of NGC 4151 itself to the neutrino signals have been studied in the literature (Inoue & Khagulyan 2023; Murase et al. 2024, but see also Peretti et al. 2023).

However, two gamma-ray loud blazars, 4FGL J1210.3+3928 and 4FGL J1211.6+3901, are located 0.08° and 0.43° respectively from NGC 4151 (Buson et al. 2023; Murase et al. 2024). While 4FGL J1210.3+3928 lies within the 68% confidence region of the neutrino excess attributed to NGC 4151, 4FGL J1211.6+3901 is located between two separated 95% confidence contours (Abbasi et al. 2024b) as shown in Fig. 1. Since blazars have been promising neutrino emitters, there might be a potential contribution from these two blazars to the observed neutrino signal attributed to NGC 4151. In this work, we in-

* e-mail: omeliukh@astro.rub.de

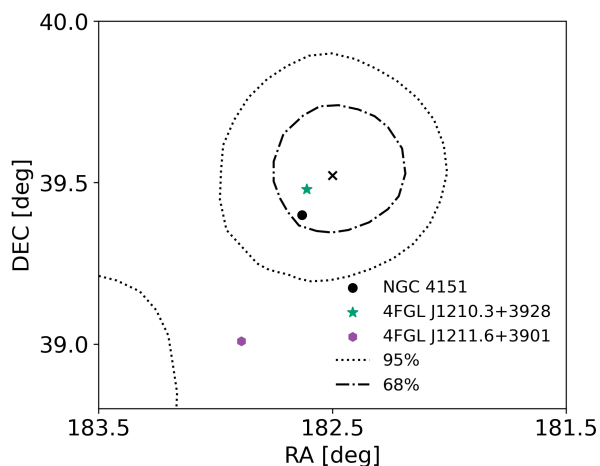


Fig. 1: The location of 4FGL J1210.3+3928 and 4FGL J1211.6+3901 with respect to NGC 4151. The black cross, dash-dotted and dotted black lines corresponds respectively to the best-fit location of the neutrino source and its 68% and 95% confidence regions (Abbasi et al. 2024b).

investigate possible contributions of these nearby blazars to the neutrino excess close to NGC 4151 by numerical modeling of the observed multi-wavelength emission of 4FGL J1210.3+3928 and 4FGL J1211.6+3901. We discuss the detectability of the predicted neutrino flux from the two blazars by next-generation neutrino telescopes. Throughout this paper, we set the cosmological constants as $H_0 = 70 \text{ km s}^{-1}$ and $\Omega_m = 0.3$.

2. Data

We collect the multi-wavelength data to build the spectral energy distribution of 4FGL J1210.3+3928 and 4FGL J1211.6+3901.

4FGL J1210.3+3928

4FGL J1210.3+3928 is a BL Lac object located at redshift $z = 0.615$ (Stocke et al. 1991). We obtain gamma-ray data from the Fermi-LAT 14-Year Point Source Catalog (4FGL-DR4; Ballet et al. 2024; Abdollahi et al. 2022). 4FGL J1210.3+3928 is detected with $\sim 6\sigma$ significance in gamma rays. The source has a gamma-ray flux of $(9 \pm 2) \times 10^{-11} \text{ erg s}^{-1}$ in the energy range of 1-100 GeV. It is well described by a power-law spectral shape with a photon index of 2.1 ± 0.2 . Its variability index is 14.42.

4FGL J1210.3+3928 is a long-term monitored source in the X-ray band due to its proximity to NGC 4151 (Maselli et al. 2008). In X-rays, 4FGL J1210.3+3928 was part of the field of view of 33 *XMM-Newton* observations between 2000 and 2022. However, due to the chosen science mode of the observations, spectra could only be extracted for 11 observations. The science products are obtained using the *XMM-Newton* Science Analysis System (SAS, Version 21.0.0). The spectra are later binned to have at least 20 counts in each bin. The extracted spectra show a flux variability of a factor 2 to 3 over the entire *XMM* observing period. For this study, we select a 10 ks observation on the 10th of December 2012 (obsID: 0679780401). This choice is motivated by two points: 1) selecting a high flux spectrum aligns with our goal to estimate the maximum neutrino emission of the source, 2) the observation date was also close to the rest of the multi-wavelength data gathered. The X-ray spectrum is well reproduced ($\chi^2/\text{dof} = 26.5/22$) by a

weakly absorbed power-law with a Hydrogen column density $N(H) = 5.5^{+3.3}_{-3.2} \times 10^{20} \text{ cm}^{-2}$ in agreement with the Galactic absorption level (HI4PI Collaboration et al. 2016) and a soft spectral index of $\Gamma = 2.19^{+0.12}_{-0.12}$. The absorbed X-ray flux in the range 0.5 to 10 keV is $3.8 \times 10^{-12} \text{ erg cm}^{-2}\text{s}^{-1}$. The spectrum is then corrected for absorption in preparation for the modeling.

For the rest of multi-wavelength data, optical data was taken from the SDSS Photometric Catalogue, Release 9 (Ahn et al. 2012). Infrared emission was measured by the Wide-field Infrared Survey Explorer (WISE) and the corresponding fluxes were taken from the WISE All-Sky Data Release (Cutri et al. 2012b,a). The source was also detected in 1.4 GHz by the FIRST Survey in 1993 (White et al. 1997).

4FGL J1211.6+3901

A second blazar, 4FGL J1211.6+3901, is classified as BL Lac object as well (Rector et al. 2000) with a redshift of $z = 0.89$ based on spectroscopic measurements by Della Ceca et al. (2015). 4FGL J1211.6+3901 is detected in gamma rays with $\sim 5.4\sigma$ significance (Ballet et al. 2024; Abdollahi et al. 2022). The source has a gamma-ray flux of $(7 \pm 2) \times 10^{-11} \text{ erg s}^{-1}$ in the energy range of 1-100 GeV and variability index of 15.52. The spectral shape follows a power law with photon index of 1.8 ± 0.2 .

We analyze the data obtained during the 15ks observation on the 14th of June 2002 by *XMM-Newton*. The blazar, which was not the main target of the observation, was at the time in an enhanced state. *XMM-Newton* data were obtained with the EPIC cameras (Strüder et al. 2001; Turner et al. 2001) in extended full-frame window mode with the medium filter applied. Science products are obtained using the *XMM-Newton* Science Analysis System (SAS, Version 21.0.0). The spectrum is later binned to have at least 20 counts in each bin. The background is found to dominate the spectrum above 7 keV, therefore we discard the energies above. The spectrum is first analyzed using XSPEC (Arnaud 1996). It is well reproduced ($\chi^2/\text{dof} = 35.7/43$) by a weakly absorbed power-law with a Hydrogen column density $N(H) = 7.9^{+4.2}_{-3.9} \times 10^{20} \text{ cm}^{-2}$ in agreement with the Galactic absorption level (HI4PI Collaboration et al. 2016) and a soft spectral index $\Gamma = 2.3^{+0.18}_{-0.17}$. The absorbed flux in the range 0.5 to 10 keV is $1.4 \times 10^{-12} \text{ erg cm}^{-2}\text{s}^{-1}$. The spectrum is then corrected for absorption in preparation for the modeling. Unfortunately, the target falls outside the field of view of the Optical Monitor (Mason et al. 2001) on-board *XMM-Newton*, and no simultaneous UV data point could be extracted.

Optical measurements were done by OSIRIS/R5000R (Della Ceca et al. 2015), Catalina Sky Survey (Drake et al. 2009), and the SDSS Photometric Catalogue, Release 12 (Alam et al. 2015). Infrared emission was measured by the Wide-field Infrared Survey Explorer (WISE) and corresponding fluxes were taken from WISE All-Sky Data Release (Cutri et al. 2012b,a). The source was also detected in 1.4 GHz by the FIRST Survey in 1993 (White et al. 1997).

3. Numerical Modeling

The spectral energy distribution (SED) of both 4FGL J1210.3+3928 and 4FGL J1211.6+3901 exhibit a black-body-like bump feature in the eV range, which does not show any significant variability (Cutri et al. 2012b,a). We consider that this feature is caused by the stellar emission from their host galaxies. A similar spectral feature is observed in the

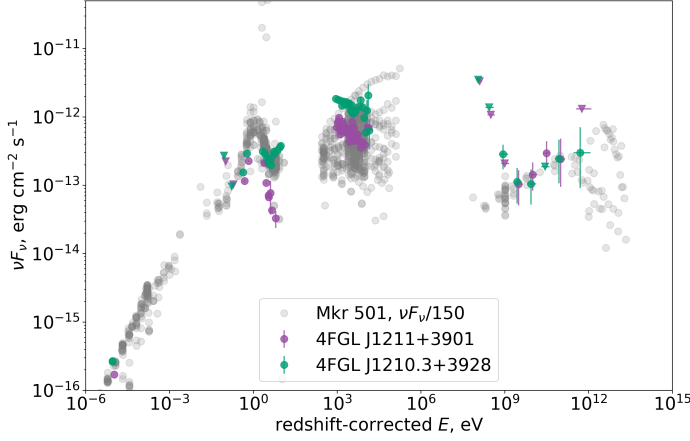


Fig. 2: Comparison between spectral energy distributions of 4FGL J1210.3+3928, 4FGL J1211.6+3901 and Mrk 501. The grey data points correspond to the archival Mrk 501 SED scaled by 150. The green and purple data points (round – measurements, triangles – upper limits) correspond to 4FGL J1211.6+3901 and 4FGL J1210.3+3928 SEDs correspondingly.

SED of Mrk 501, a prototype high-synchrotron-peaked BL Lac (HBL) object. A comparison of the rest frame SEDs of these blazars with Mrk 501¹ is shown in Fig. 2. The similarity in their broad-band spectral properties confirms the classification of both sources as typical HBLs. The eV bumps in both blazars are well reproduced by an elliptical galaxy spectral template with a stellar mass of $M = 10^{12} M_{\odot}$. We adopt the stellar population synthesis model by (Bruzual & Charlot 2003) assuming the Salpeter initial mass function, instantaneous star formation, age of 10 Gyr, and solar metallicity (see Itoh et al. 2020, for details).

For each state, we numerically model multi-wavelength emission using the time-dependent code AM³ (Klinger et al. 2023), which solves a system of coupled differential equations describing the transport of particles interacting in the jet in a self-consistent way. Motivated by the possible neutrino emission, we start with a model where all radiation² originates from radiation processes of electrons and protons in the jet. We assume that both electrons and protons are accelerated in the source to power-law spectra³ $dN/d\gamma'_{e,p} \propto \gamma'^{-\alpha_{e,p}}$ with spectral indices $\alpha_{e,p}$, spanning a range of Lorentz factors from $\gamma'_{e,p}^{\min}$ to $\gamma'_{e,p}^{\max}$. The energy spectra of the electrons and protons are normalized to the corresponding total electron and proton luminosities, L'_e and L'_p . These particles are then injected into a single spherical blob of size R' (in the comoving frame of the jet) moving along the jet with Lorentz factor Γ , where there is a homogeneous and isotropic magnetic field of strength B' . We assume the jet is observed at an angle $\theta_{\text{obs}} = 1/\Gamma_b$ relative to its axis, resulting in a Doppler factor of $\delta_D \approx \Gamma_b$. We account for the high-energy gamma-ray absorption due to extragalactic background light (EBL) using the model

¹ The Mrk 501 SED data was obtained through the SEDBuilder tool <https://tools.ssdc.asi.it/SED/>

² Radio fluxes cannot be explained within the one-zone model framework since the compact region is optically thick to low-frequency radio emission due to synchrotron self-absorption.

³ Parameters with or without prime refer to the values in the jet or observer's frame respectively.

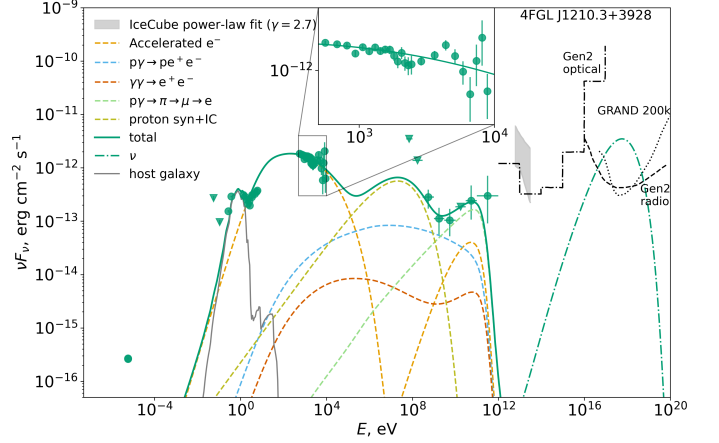


Fig. 3: Leptohadronic model for 4FGL J1210.3+3928. The green solid line correspond to the multi-wavelength photon emission. The components are shown with dashed line. The green dash-dotted line corresponds to the neutrino spectrum. The grey shaded area is a neutrino flux from NGC 4151 under the assumption of power-law with spectral index $\gamma = 2.7$ (Abbasi et al. 2024a). The black dash-dotted line shows 10 year sensitivity of IceCube-Gen2 optical array (Aartsen et al. 2021), black dashed – 10 year sensitivity of IceCube-Gen2 radio array (Aartsen et al. 2021), black dotted line – 10 year sensitivity of GRAND 200k (Álvarez-Muñiz et al. 2020).

by Domínguez et al. (2011). The best-fit parameter values were found by minimizing the reduced χ^2 with the Minuit package (James & Roos 1975). The results of the leptohadronic modeling for 4FGL J1210.3+3928 and 4FGL J1211.6+3901 are shown in Fig. 3 and Fig. 4 respectively. The values of the leptohadronic parameters can be found in Table A.1.

As an alternative scenario, we also consider a case where all radiation originates from purely leptonic processes. We assume that electrons are accelerated to a single power-law spectrum $dN/d\gamma'_e \propto \gamma'^{-\alpha_e}$ with spectral index α_e , spanning a range of Lorentz factors from γ'_e^{\min} to γ'_e^{\max} . The energy spectrum of the electrons is normalized to the total electron luminosity parameter, L'_e . Similarly to the leptohadronic case, electrons undergo interactions and radiate inside of a spherical blob of size R' with a homogeneous and isotropic magnetic field of strength B' moving along the jet with Lorentz factor Γ . The obtained best-fit solutions for both sources are shown in Fig. 5.

4. Results

The best-fit values of the leptohadronic models for both sources have typical values for HBL sources (Rodrigues et al. 2024). The characteristic size of the emission zone is 5×10^{16} cm with a magnetic field strength of 0.05 – 0.1 G. Both sources require the presence of a high-energy electron population (with Lorentz factors ranging from $\sim 10^4$ to $\sim 10^6$) in order to explain the optical and X-ray fluxes. To produce neutrinos, highly relativistic protons must be present in the jet. The maximum proton energy in the obtained models is $\sim 10^{18}$ eV for 4FGL J1210.3+3928 and $\sim 10^{17}$ eV for 4FGL J1211.6+3901 which correspond to the energies of ultra-high-energy cosmic rays (UHECR). Similar values for the maximum proton energies were predicted for a different HBL, Mrk 421, in Dimitrakoudis et al. (2014).

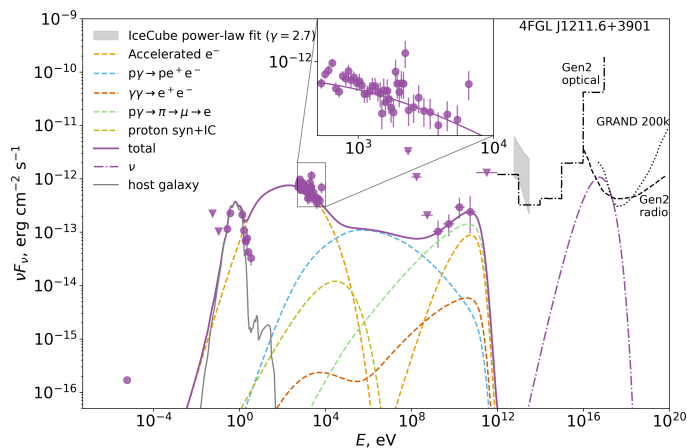


Fig. 4: Leptohadronic model for 4FGL J1211.6+3901. The purple solid line correspond to the multi-wavelength photon emission. The components are shown with dashed line. The purple dash-dotted line corresponds to the neutrino spectrum. The grey shaded area is a neutrino flux from NGC 4151 under the assumption of power-law with spectral index $\gamma = 2.7$ (Abbasi et al. 2024a). The black dash-dotted line shows 10 year sensitivity of IceCube-Gen2 optical array (Aartsen et al. 2021), black dashed – 10 year sensitivity of IceCube-Gen2 radio array (Aartsen et al. 2021), black dotted line – 10 year sensitivity of GRAND 200k (Álvarez-Muñiz et al. 2020).

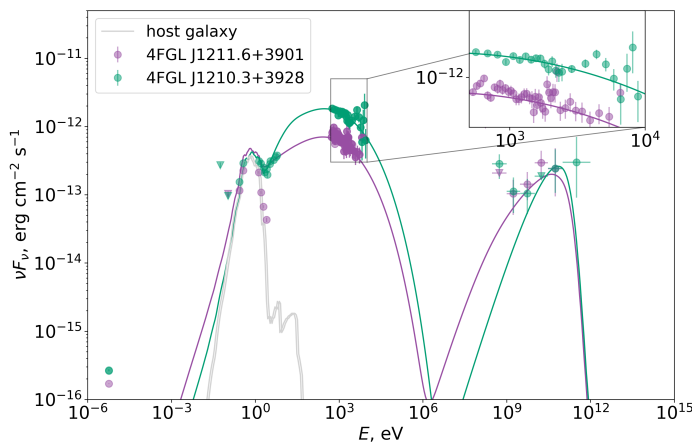


Fig. 5: Leptonic models for both quiescent (blue) and flaring (red) states. The solid line correspond to the multi-wavelength photon emission. The solid grey line corresponds to the emission of the host galaxy.

The gamma-ray spectrum of 4FGL J1210.3+3928 exhibits a distinctive dip in the GeV range (Fig. 3). This spectral feature is successfully reproduced by our leptohadronic model, which combines proton-synchrotron emission (\lesssim GeV) of with photopion production (\gtrsim GeV). In contrast, purely leptonic scenarios fail to explain this spectral characteristic through inverse-Compton emission alone (Fig. 5).

In the case of 4FGL J1211.6+3901, both leptonic and leptohadronic models describe the observed gamma-ray, X-ray and near-infrared fluxes well. The discrepancy in the optical band for

both models can be caused by non-simultaneous data, which is important to account for effects of source variability. Unfortunately, with the limited optical data, no simultaneous SED could be built. We note that with the currently available data, there are no possibilities to discriminate between purely leptonic and leptohadronic scenario. An important energy region that can shed light on this problem is MeV gamma rays. High-energy photons passing in the vicinity of protons produce Bethe-Heitler pairs, which in turn also emit synchrotron radiation which peaks in the MeV range. This excess of MeV photons can be a hadronic signature which highlights the importance of future MeV Compton telescopes such as COSI (Tomsick et al. 2019), GRAMS (Arakami et al. 2020), and AMEGO-X (Caputo et al. 2022).

Our leptohadronic modeling predicts neutrino fluxes of $\sim 10^{-12}$ erg cm $^{-2}$ s $^{-1}$ peaking above ~ 10 PeV for both blazars. These predicted fluxes suggest that the contribution of these sources to the neutrino signal observed by IceCube in the direction of NGC 4151 is minor. As shown in Figs. 3 and 4, despite the improved PeV-range sensitivity of the optical array in the next-generation neutrino observatory IceCube-Gen2 (Aartsen et al. 2021), detection of PeV neutrinos from these blazars remains challenging. Detection of neutrinos at 10^{17} eV, where the emission peaks, requires either the radio array of IceCube-Gen2 or a detector like GRAND (Álvarez-Muñiz et al. 2020). The predicted neutrino emission from 4FGL J1210.3+3928 should be detectable by both facilities. The neutrino flux from 4FGL J1211.6+3901 lies at the edge of GRAND 200k’s 10-year sensitivity and slightly above the 10-year sensitivity of IceCube-Gen2’s radio array, suggesting possible detection with IceCube-Gen2. We note that the accuracy of the directional reconstruction is expected to be better than 1° for the IceCube-Gen2 radio array (Aartsen et al. 2021) and better than 0.5° for GRAND (Álvarez-Muñiz et al. 2020). In case of the detection of multiple neutrinos, these values can be further improved, leading to a possible spatial separation of signals from 4FGL J1210.3+3928 and 4FGL J1211.6+3901.

5. Discussion and Conclusions

The IceCube analysis has found around 30 signal neutrinos from NGC 4151 in 10 years of data (Abbasi et al. 2024a). However, two gamma-ray bright blazars, 4FGL J1210.3+3928 and 4FGL J1211.6+3901, are located 0.08° and 0.43° from NGC 4151 respectively. Blazars are promising neutrino emitters and can contribute to the observed IceCube signal. We modeled the multi-wavelength spectrum of both blazars. The leptohadronic model of 4FGL J1210.3+3928 explained the observed electromagnetic fluxes including a GeV dip in gamma rays, which can be explained by a purely leptonic model. For 4FGL J1211.6+3901, both leptonic and leptohadronic models explain the observed data equally well. We found that the predicted neutrino flux peaks around 10^{17} eV for both sources, as expected for HBLs. The contribution to the observed TeV neutrino flux is expected to be subdominant.

Both 4FGL J1210.3+3928 and 4FGL J1211.6+3901 have high-energy synchrotron peaks in X-ray, indicating the presence of efficient particle acceleration. In our model, the neutrino spectrum peaks at ~ 100 PeV due to $p\gamma$ interactions with internal synchrotron photons and the extension of cosmic-ray spectra to EeV energies. While lowering the maximum proton energy could shift the neutrino peak toward TeV energies (Dermer et al. 2014), where IceCube detected neutrinos from the direction of NGC 4151, such models would require substantially higher pro-

ton powers and fail to explain the observed broad-band electromagnetic spectra. This demonstrates the robustness of our solution within the large parameter space of one-zone radiation models, despite potential degeneracies in the model parameters (Omeliukh et al. 2024).

The proton luminosity is fundamentally limited by the accretion power. Since we do not have the measurements of accretion powers in these blazars, we follow the Eddington power argument. We can do an order-of-magnitude Eddington luminosity estimation using the relation between black hole mass and bulk mass (e.g. Häring & Rix 2004; Zhu et al. 2021). Based on our fitted galactic profile, $M_{\text{bulk}} = 10^{12} M_{\odot}$ which roughly corresponds to $M_{\text{BH}} = 10^9 M_{\odot}$ leading to $L_{\text{Edd}} \sim 10^{47}$ erg/s. When lowering the maximum proton energy to $10^{15} - 10^{16}$ eV and setting the proton luminosity to the Eddington luminosity, the neutrino spectrum is still expected to peak above PeV energies and thus the blazar contribution to the neutrino signal from the region near NGC 4151 can be only subdominant.

Models for neutrino emission from the Seyfert galaxy NGC 4151 predict neutrinos at lower energies compared to our models for the two nearby blazars. While most of the models predict a cut-off of the neutrino spectrum above 10-100 TeV for Seyfert galaxies, HBLs can produce neutrinos at higher energies. Next generation neutrino telescope such as IceCube-Gen2 or GRAND may be able to solve this discrepancy by probing a higher energy range and possibly spatially discriminating two hotspots. In addition, future MeV gamma-ray missions will be able to test signatures of hadronic emission.

Acknowledgements. The authors thank Anna Franckowiak for useful comments and discussions. AO is supported by DAAD funding program 57552340 and RUB Research School. AO acknowledges the support from the DFG via the Collaborative Research Center SFB1491 Cosmic Interacting Matters - From Source to Signal. SB is an overseas researcher under the Postdoctoral Fellowship of Japan Society for the Promotion of Science (JSPS), supported by JSPS KAKENHI Grant Number JP23F23773. YI is supported by NAOJ ALMA Scientific Research Grant Number 2021-17A; by World Premier International Research Center Initiative (WPI), MEXT; and by JSPS KAKENHI Grant Number JP18H05458, JP19K14772, and JP22K18277.

References

Aartsen, M. G., Abbasi, R., Ackermann, M., et al. 2021, *Journal of Physics G Nuclear Physics*, 48, 060501

Aartsen, M. G., Ackermann, M., Adams, J., et al. 2020, *Phys. Rev. Lett.*, 124, 051103

Abbasi, R., Ackermann, M., Adams, J., et al. 2024a, arXiv e-prints, arXiv:2406.07601

Abbasi, R., Ackermann, M., Adams, J., et al. 2024b, arXiv e-prints, arXiv:2406.06684

Abdollahi, S., Acero, F., Baldini, L., et al. 2022, *The Astrophysical Journal Supplement Series*, 260, 53

Ahn, C. P., Alexandroff, R., Allende Prieto, C., et al. 2012, *ApJS*, 203, 21

Alam, S., Albareti, F. D., Allende Prieto, C., et al. 2015, *ApJS*, 219, 12

Álvarez-Muñiz, J. et al. 2020, *Sci. China Phys. Mech. Astron.*, 63, 219501

Aramaki, T., Adrian, P. O. H., Karagiorgi, G., & Odaka, H. 2020, *Astroparticle Physics*, 114, 107

Arnaud, K. A. 1996, in *Astronomical Society of the Pacific Conference Series*, Vol. 101, *Astronomical Data Analysis Software and Systems V*, ed. G. H. Jacoby & J. Barnes, 17

Ballet, J., Bruel, P., Burnett, T. H., Lott, B., & collaboration, T. F.-L. 2024, *Fermi Large Area Telescope Fourth Source Catalog Data Release 4 (4FGL-DR4)*

Bruzual, G. & Charlot, S. 2003, *MNRAS*, 344, 1000

Buson, S., Tramacere, A., Oswald, L., et al. 2023, arXiv e-prints [arXiv:2305.11263]

Caputo, R., Ajello, M., Kierans, C. A., et al. 2022, *Journal of Astronomical Telescopes, Instruments, and Systems*, 8, 044003

Cutri, R. M., Wright, E. L., Conrow, T., et al. 2012a, *Explanatory Supplement to the WISE All-Sky Data Release Products*, *Explanatory Supplement to the WISE All-Sky Data Release Products*

Cutri, R. M. et al. 2012b, *VizieR Online Data Catalog: WISE All-Sky Data Release (Cutri+ 2012)*, *VizieR On-line Data Catalog: II/311*.

Della Ceca, R., Carrera, F. J., Caccianiga, A., et al. 2015, *Monthly Notices of the Royal Astronomical Society*, 447, 3227

Dermer, C. D., Murase, K., & Inoue, Y. 2014, *Journal of High Energy Astrophysics*, 3, 29

Dimitrakoudis, S., Petropoulou, M., & Mastichiadis, A. 2014, *Astroparticle Physics*, 54, 61

Domínguez, A., Primack, J. R., Rosario, D. J., et al. 2011, *MNRAS*, 410, 2556

Drake, A. J., Djorgovski, S. G., Mahabal, A., et al. 2009, *ApJ*, 696, 870

Franckowiak, A., Garrappa, S., Paliya, V., et al. 2020, *The Astrophysical Journal*, 893, 162

Gao, S., Pohl, M., & Winter, W. 2017, *ApJ*, 843, 109

Garrappa, S., Buson, S., Franckowiak, A., et al. 2019, *ApJ*, 880, 103

Häring, N. & Rix, H.-W. 2004, *ApJ*, 604, L89

HI4PI Collaboration, Ben Bekhti, N., Flöer, L., et al. 2016, *A&A*, 594, A116

IceCube Collaboration. 2013, *Science*, 342, 1242856

IceCube Collaboration, Abbasi, R., Ackermann, M., et al. 2022, *Science*, 378, 538

IceCube Collaboration, Fermi-LAT, MAGIC, et al. 2018, *Science*, 361, eaat1378

Inoue, Y. & Khangulyan, D. 2023, *Publ. Astron. Soc. Jap.*, 75, L33

Inoue, Y., Khangulyan, D., Inoue, S., & Doi, A. 2019, *ApJ*, 880, 40

Itoh, R., Utsumi, Y., Inoue, Y., et al. 2020, *Astrophys. J.*, 901, 3

James, F. & Roos, M. 1975, *Computer Physics Communications*, 10, 343

Kadler, M., Krauß, F., Mannheim, K., et al. 2016, *Nature Physics*, 12, 807

Klinger, M., Rudolph, A., Rodrigues, X., et al. 2023, *AM³: An Open-Source Tool for Time-Dependent Lepto-Hadronic Modeling of Astrophysical Sources*

Maselli, A., Giommi, P., Perri, M., et al. 2008, *A&A*, 479, 35

Mason, K. O., Breeveld, A., Much, R., et al. 2001, *A&A*, 365, L36

Murase, K., Karwin, C. M., Kimura, S. S., Ajello, M., & Buson, S. 2024, *Astrophys. J. Lett.*, 961, L34

Neronov, A., Savchenko, D., & Semikoz, D. V. 2024, *Phys. Rev. Lett.*, 132, 101002

Omeliukh, A., Garrappa, S., Fallah Ramazani, V., et al. 2024, arXiv e-prints, arXiv:2409.04165

Peretti, E., Peron, G., Tombesi, F., et al. 2023, arXiv e-prints, arXiv:2303.03298

Rector, T. A., Stocke, J. T., Perlman, E. S., Morris, S. L., & Gioia, I. M. 2000, *The Astronomical Journal*, 120, 1626

Rodrigues, X., Garrappa, S., Gao, S., et al. 2021, *The Astrophysical Journal*, 912, 54

Rodrigues, X., Paliya, V. S., Garrappa, S., et al. 2024, *A&A*, 681, A119

Sahakyan, N., Giommi, P., Padovani, P., et al. 2022, *Monthly Notices of the Royal Astronomical Society*, 519, 1396

Sommani, G., Franckowiak, A., Lincetto, M., & Dettmar, R.-J. 2024, *Two 100 TeV neutrinos coincident with the Seyfert galaxy NGC 7469*

Stocke, J. T., Morris, S. L., Gioia, I. M., et al. 1991, *ApJS*, 76, 813

Strüder, L., Briel, U., Dennerl, K., et al. 2001, *A&A*, 365, L18

Tomsick, J., Zoglauer, A., Slesator, C., et al. 2019, in *Bulletin of the American Astronomical Society*, Vol. 51, 98

Turner, M. J. L., Abbey, A., Arnaud, M., et al. 2001, *A&A*, 365, L27

White, R. L., Becker, R. H., Helfand, D. J., & Gregg, M. D. 1997, *ApJ*, 475, 479

Yuan, W., Fausnaugh, M. M., Hoffmann, S. L., et al. 2020, *The Astrophysical Journal*, 902, 26

Zhu, P., Ho, L. C., & Gao, H. 2021, *The Astrophysical Journal*, 907, 6

Appendix A: Model parameters

Table A.1: Table of best-fit parameters for leptonic and leptohadronic models during the quiescent and flaring states of J1211.6+3901

| Parameters | 4FGL J1210.3+3928 leptohadronic | 4FGL J1211.6+3901 leptohadronic | 4FGL J1210.3+3928 leptonic | 4FGL J1211.6+3901 leptonic |
|--------------------|------------------------------------|------------------------------------|-------------------------------|-------------------------------|
| R'_b [cm] | 5×10^{16} | 5×10^{16} | 3×10^{16} | 3.5×10^{16} |
| B' [G] | 0.1 | 0.04 | 0.05 | 0.04 |
| Γ_b | 25 | 25 | 25 | 25 |
| $\gamma'_{e,\min}$ | 2×10^4 | 2×10^4 | 2.5×10^4 | 1×10^4 |
| $\gamma'_{e,\max}$ | 1×10^6 | 1×10^6 | 1×10^6 | 1×10^6 |
| α'_e | 2.0 | 2.3 | 2.3 | 2.3 |
| L'_e [erg/s] | 3×10^{40} | 7.5×10^{40} | 7×10^{40} | 1.3×10^{41} |
| $\gamma'_{p,\min}$ | 2×10^3 | 2×10^3 | – | – |
| $\gamma'_{p,\max}$ | 1.5×10^9 | 6×10^7 | – | – |
| α'_p | 1.9 | 1.5 | – | – |
| L'_p [erg/s] | 4×10^{45} | 1.5×10^{46} | – | – |